Mathematical Abilities in Children: An sMRI Analysis With Radiomics

Violeta Pina
Universidad de Granada
Víctor M Campello
Universitat de Barcelona
Karim Lekadir
Universitat de Barcelona
Santi Seguí
Universitat de Barcelona
José María García Santos
Hospital General Universitario Jose M Morales Meseguer
Luis J Fuentes (lfuentes@um.es)
Universidad de Murcia https://orcid.org/0000-0002-3203-9976

Research Article

Keywords: Children, Machine Learning, Mathematical Performance, Radiomics, sMRI

Posted Date: April 13th, 2021

DOI: https://doi.org/10.21203/rs.3.rs-406108/v1

Noname manuscript No.
(will be inserted by the editor)

Mathematical abilities in children: an sMRI analysis with radiomics

Violeta Pina · Víctor M. Campello · Karim Lekadir · Santi Seguí · José María García-Santos · Luis J. Fuentes

the date of receipt and acceptance should be inserted later

Abstract Brain areas related to mathematical abilities in children have been mainly assessed through their activation in fMRI, while volume-based analysis have been employed in sMRI to discover structural differences. However, a recent technique in precision medicine allows to enhance the sMRI analysis by extracting a large number of features, also called radiomics, related to shape, intensity and texture from specific areas. In the present study, a structural neuroimaging analysis based on radiomics and machine learning models is presented with the aim of identifying brain areas related to different mathematical tests. A total of 77 school-aged children from third to sixth grade were administered four mathematical tests: Math Fluency, Calculation, Applied Problems and Concepts as well as a structural brain imaging scan. The results confirmed and extended the involvement of brain areas found in sMRI and fMRI literature such as the frontal, parietal, temporal and occipital cortex, as well as basal ganglia and limbic system areas. For these areas, texture features were the most informative while volume represented less than 15% of the shape information. These findings emphasize the potential of radiomics for a more in-depth analysis of medical images for the identification of brain areas related to mathematical performance. The code used to obtain these results can be found at github.com/vicmancr/MathBrainRadiomics.

Keywords Children · Machine Learning · Mathematical Performance · Radiomics · sMRI

V. Pina
Faculty of Education, Economics and Technology in Ceuta. University of Granada. Cortadura del Valle s.n., 51001 Ceuta, Spain.

V. M. Campello · K. Lekadir · S. Seguí
Departament de Matemàtiques i Informàtica. Universitat de Barcelona. Gran Via de les Corts Catalanes, 585, 08007 Barcelona, Spain.

J. M. García-Santos
Radiology Service. Morales Meseguer Hospital. Av. Marqués de los Vélez s.n., 30008 Murcia, Spain.

L. J. Fuentes
Faculty of Psychology. University of Murcia. Campus Universitario de Espinardo, 30100 Murcia, Spain.
E-mail: lfuentes@um.es

Abbreviations

MAE	Mean Absolute Error
RF	Random Forest
VBM	Voxel-Based Morphometry

Introduction

Recent research has focused on determining the cognitive processes that are associated with mathematical performance, as well as the brain areas involved. The goal is not only to reach a more comprehensive understanding of how children and adults solve mathematical problems but also to better characterize disorders that affect mathematical abilities.

A bulk of evidence is currently available showing crucial brain areas related to mathematical abilities, with functional magnetic resonance imaging (fMRI) studies outweighing structural magnetic resonance imaging (sMRI) ones (Peters and Smedt 2017). fMRI studies have revealed active parietal and frontal areas, involved in attention and working memory (WM) when children perform mathematical tasks (Eriksson et al. 2015; Gazzaley et al. 2004). For instance, the right parietal lobe along with the cingulate gyrus and frontal areas, such as

the left superior frontal gyrus, left inferior frontal gyrus (IFG), and right medial frontal gyrus (MFG), would be involved in calculation tasks, whereas the insula and claustrum are related to intrinsic motivation when performing mathematical tasks that require attentional effort (Arsalidou et al. 2017; Houdé et al. 2010). The relationship between attention/working memory and mathematical performance has further been established in some cognitive-training studies with children (Sánchez-Pérez et al. 2018).

Similar findings have also been reported with sMRI. Recent voxel-based morphometry (VBM) approaches, which measure the volume of white and gray matter, found that children with poor mathematical abilities showed reduced gray matter volume in several brain areas related to number processing, attentional control, and memory, such as the posterior parietal cortex, including the intraparietal sulcus (IPS), frontal areas such as IFG and MFG, hippocampal areas, and occipito-temporal areas (Fritz et al. 2019; Peters and Smedt 2017). Also, VBM has revealed that reduced gray matter in the left IPS, an area that is involved in attention, numerical processing and working memory, is associated with higher levels of mathematical anxiety (Hartwright et al. 2018). However, VBM techniques are prone to registration errors and inter-subject variability.

In the present study a radiomics approach is investigated for deeper analysis. Radiomics refers to a type of image analysis mainly applied in the field of precision medicine, that allows researchers to perform a more exhaustive analysis of medical images, by computing and mining a large pool (thousands) of advanced imaging features (Gillies et al. 2016). Thus far, radiomics-based analyses have been carried out mostly in oncology, and more recently for lung and cardiovascular applications (Guerrisi et al. 2020; Huang et al. 2016; Raisi-Estabragh et al. 2020). To date, few studies have explored this technique in the area of psychology (Chaddad et al. 2017; Sun et al. 2018; Cui et al. 2020). sMRI based techniques applied to mathematical performance have focused primarily on the analysis of volumetric measures, whereas radiomics includes additional shape and texture features that may provide extra value for the identification of brain areas involved in predicting children's mathematical abilities. Here, we describe a radiomics-based approach to identify the structural brain areas involved in different mathematical abilities in school-aged children.

Materials and methods

Participants

One hundred and four 7 to 12 year-old children that participated in a larger project (Sánchez-Pérez et al. 2018), took part in the present neuroimaging study. Children were recruited from two primary education schools in the Región de Murcia (Spain), and were enrolled in grades 3 to 6. Data were collected from mathematical standardized tests and sMRI. The final sample reduced to 77 children (43 boys and 34 girls, mean age 9.7; SD 1.2), after excluding: data with excessive motion, children that refused to enter into the scanner at the moment of scanning, or equipment failures. The K-Bit test (Kaufman and Kaufman 1990) was administered to verify that all children had average intelligence. Children with special educational needs were not included in the overarching study.

The project was approved by the Ethics Committee of the University of Murcia and it was conducted in accordance with the approved guidelines and the Declaration of Helsinki. Written informed consent was obtained from the parents, and oral consent from the children at the moment of scanning.

Behavioral data

Mathematical ability tests. Children's math abilities were assessed through the Woodcock-Johnson III (WJ-III) Achievement battery for children aged 6 to 13 years in Spain (Diamantopoulou et al. 2012). It comprises four tests: Math Fluency, Calculation, Applied Problems, and Quantitative Concepts. Descriptive data are shown in Table 1. Math Fluency measures the ability to quickly solve a total of 160 simple addition, subtraction, and multiplication within 3 minutes. Calculation measures the ability to perform simple mathematical computations including 46 ascending difficulty addition, subtraction, multiplication, and division. Applied Problems measures the ability to analyze and solve 62 ascending difficulty math word problems. Quantitative Concepts measures the knowledge about mathematical concepts, symbols, vocabulary and numerical series in 57 items (Pina et al. 2015; Sánchez-Pérez et al. 2018). The scoring for all items was 0 (incorrect) and 1 (correct). The final score for each subtest is the sum of all correct answers.

Table 1: Descriptors for the mathematical ability tests considered in this study. Values are presented as mean (standard deviation).

Grade	Boys/ Girls	Age	Math Fluency	Calculation	Applied Problems	Concepts
3	9/15	8.5 (0.33)	37.6 (6.9)	13.0 (2.4)	29.7 (3.0)	16.9 (2.1)
4	15/9	9.4 (0.39)	46.5 (11.3)	16.8 (2.1)	33.8 (4.4)	19.4 (2.8)
5	12/5	10.6 (0.37)	62.4 (18.6)	18.4 (1.8)	35.8 (3.5)	20.6 (1.6)
6	7/5	11.6 (0.27)	63.3 (19.6)	19.3 (2.1)	39.3 (5.2)	22.8 (2.1)
All	43/34	9.7 (1.15)	49.9 (17.2)	16.3 (3.2)	33.8 (5.1)	19.4 (3.0)

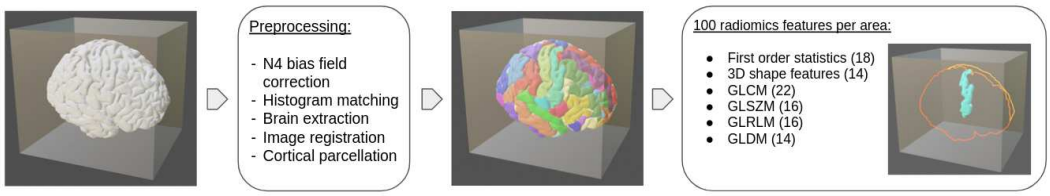

Fig. 1: Schematic pipeline for extracting radiomics features from sMRI.

Image Acquisition

Anatomical MRI data were acquired using a General Electric 1.5 T HDX scanner in the Hospital General Universitario Morales Meseguer (Murcia). A parent was present with the child during scanning and earplugs were used for protecting the child's hearing. Soft pads were used to reduce motion artifacts. The sequence parameters were as follows: TR, 12.4 ms; TE, 5.2-15 ms; voxel size, 1x1x1 mm; flip angle, 12º; 142 axial slices (Sánchez-Pérez et al. 2019).

Image Analysis

Several pre-processing steps were conducted prior to the cortical parcellation and features extraction (see Figure 1). First of all, possible low frequency intensity inhomogeneities were corrected using N4 Bias Field correction (SimpleITK, version 1.2.4, Lowekamp et al. 2013). Then, image intensities were standardized using histogram matching for the whole volume with a reference participant selected visually (scikit-image, version 0.18.1). Finally, three-dimensional image registration was used to transform the images to a common space with Advanced Normalization Tools (ANTs, version 0.2.2, Tustison et al. 2014) for Python. The preprocessed images were then used to extract and parcellate the brain with the Freesurfer package (version 6, Fischl et al. 2004) according to the Destrieux Atlas (Destrieux et al. 2010). For each of the 191 extracted brain areas, a set of 100 radiomics features were computed accounting for its shape, intensity and texture using the PyRadiomics library (version 2.2.0, Griethuysen et al. 2017) with the default configuration (bin width of 25). To see the complete list of extracted features see Table 3 in the supplementary material.

Machine learning-based area ordering

In order to discover which brain areas are more involved for the mathematical tests under consideration, a regression-based analysis, with age as control variable, is proposed for predicting the final subtest score. For each regression and for each area, a prediction error is extracted using the absolute deviation from the real score (Mean Absolute Error, MAE), allowing the ordering of areas from more to less predictive.

A Random Forest (RF) regression model is proposed to account for linear and non-linear relations of brain areas characteristics with mathematical abilities. This model reduces the prediction variance while preventing over-fitting with the increase of decision trees, becoming optimal for this dataset. Default values were used as hyperparameters for each model (100 decision trees, as in scikit-learn version 0.22.1), but for a maximum of 5 decision steps to prevent decision trees from being too specific for the training sample. Due to the rather small sample size and the large input feature space, a feature selection was conducted for each area during training. The final set of variables were selected sequentially, one by one. At each step, we removed the variables that had a squared correlation coefficient over 0.8 with the selected variable (see Figure 2). The final selected features accounted for a percentage in between 81% and 39% of the initial features, depending on the area under

consideration. The selected features together with age were used as input variables.

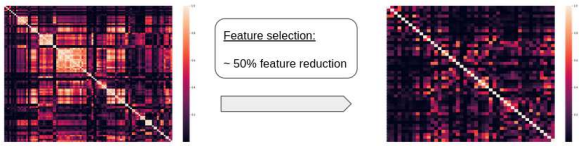

Fig. 2: Example of a correlation matrix for radiomics features before and after the feature reduction for a given area, showing significant reduction in the number of correlated features.

For each test and each area, the following pipeline was used to ensure the robustness of the final results (see Figure 3): (1) 20 random partitions of the dataset in training (80%) and testing (20%) were generated, (2) 100 different RF regression models were trained on each partition and the median MAE was extracted, and (3) the resulting MAE was obtained as the median across the 20 partitions. The median was chosen over the mean due to its robustness against outliers.

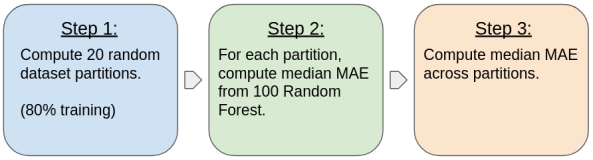

Fig. 3: Method pipeline used for computing the resulting errors for each area and for each mathematical test.

Results

For each mathematical test the most predictive and significant areas were selected. To do this, the resulting mean absolute errors (MAEs) were assumed to follow a normal distribution and those areas with an error below two standard deviations from the mean ($p < 0.022$) were classified as "most relevant". Then, the p-value associated to these areas was obtained comparing their performance against the noise distribution, obtained with the same methodology using random features as input variables. Results below three standard deviations from the noise distribution mean ($p < 0.01$) were classified as significant. Table 2 summarizes the final selected areas for each test.

For the Math Fluency test (Figure 4a), five areas were found below the two-sigma threshold with high significance ($ps < 0.0014\%$), involving the two brain hemispheres. In particular, the right lateral sulcus (sylvian fissure), the left intraparietal sulcus and the right postcentral gyrus in the parietal lobe and the middle frontal sulci bilaterally.

For the Calculation test (Figure 4b), five areas were selected with a significance level ps between 0.0052 and 0.0015 from both hemispheres. The most relevant region was the left accumbens area, followed by the left middle cingulate gyrus and sulcus, the right suborbital sulcus, the right cuneus gyrus and the right postcentral gyrus .

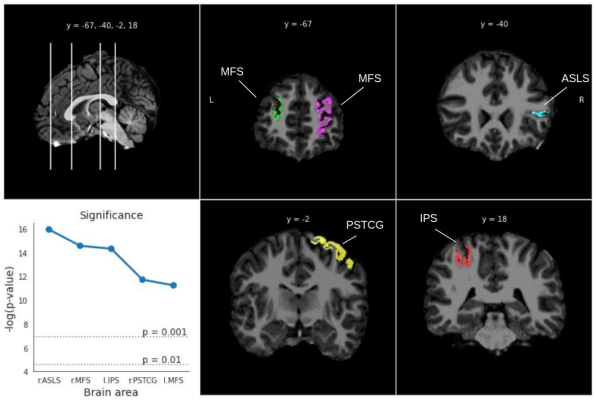

(a) Results for the math fluency test.

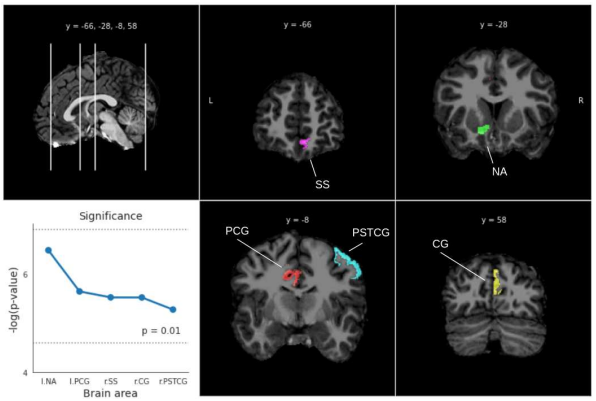

(b) Results for the calculation test.

Fig. 4: Significant areas for math fluency and calculation tests with corresponding plots of the logarithmic p-values for each area. The acronyms are defined in Table 2.

For the Applied Problems test (Figure 5a), two very significant regions were obtained ($ps < 0.000013\%$). In particular, the right rectus gyrus and the right inferior frontal gyrus were found.

Finally, for the Concepts test (Figure 5b), three areas from the left hemisphere were found with significance levels below 0.0029. In particular, the parahip-

Table 2: Predictive areas of math performance in the four tests of the WJ-III battery.

Test	Atlas label	H	Loc	Area name - Acronym	P-value
Math Fluency	12140	R	IF	Vertical ramus of the anterior segment of the lateral sulcus (or fissure) - ASLS	1.2×10^{-7}
	12154	R	MF	Middle frontal sulcus - MFS	4.7×10^{-7}
	11157	L	PL	Intraparietal sulcus and transverse parietal sulci - IPS	6.1×10^{-7}
	12128	R	PL	Post central gyrus - PSTCG	8.1×10^{-6}
	11154	L	MF	Middle frontal sulcus - MFS	1.3×10^{-5}
Calculation	26	L	BG	Nucleus accumbens - NA	1.5×10^{-3}
	11108	L	LS	Middle-posterior part of the cingulate gyrus and sulcus - PCG	3.6×10^{-3}
	12171	R	FL	Suborbital sulcus (sulcus rostrales, supraorbital sulcus) - SS	4.0×10^{-3}
	12111	R	OL	Cuneus gyrus - CG	4.0×10^{-3}
	12128	R	PL	Post central gyrus - PSTCG	5.1×10^{-3}
Applied Problems	12131	R	IF	Straight gyrus, Gyrus rectus - SG	7.4×10^{-10}
	12113	R	IF	Orbital part of the inferior frontal gyrus - OIFG	1.2×10^{-5}
Concepts	11123	L	LS	Parahippocampalgyrus, parahippocampal part of the medial occipito-temporal gyrus - PHPG	3.0×10^{-4}
	11125	L	PL	Angular gyrus - AG	1.7×10^{-3}
	11133	L	TL	Anterior transverse temporal gyrus (of Heschl) - HG	2.8×10^{-3}

H and Loc stand for Hemisphere and Localization, respectively. Localization: IF (inferior Frontal), MF (middle frontal), PL (parietal lobe), BG (basal ganglia), LS (limbicsystem), FL (frontal lobe), OL (occipital lobe), TL (temporal lobe).

pocampal gyrus was the most relevant area, followed by the angular gyrus and Hesch gyrus.

In order to find out the relevance of each type of features for each of the brain areas analyzed, the Gini importance for age, shape, intensity, and texture features was calculated (see Figure 6). The area volume, used mainly in VBM, was considered apart from shape features, to assess its contribution independently. Our results show that texture features provide more information about areas, followed by shape and intensity features. Importantly, volume represents less than 15% of the shape features contribution in all cases.

Discussion

Most of sMRI studies that have explored the brain areas involved in mathematical abilities used mainly volume. However, by using a radiomics-based analysis we have demonstrated that volume contribution to identify the brain areas that predict children's math abilities is minimal compared with texture, shape and intensity measures. In particular, texture features are the most informative variables per area in our analysis. These features quantify the local heterogeneity of tissues often unrecognizable through visual assessment (Larroza et al. 2016) and have been found to be important biomarkers for cognitive traits such as autism spectrum disorder (Chaddad et al. 2017) or schizophrenia (Park et al. 2020).

Until now, fewer studies have used sMRI volume analysis in mathematical abilities and these have provided less information than fMRI activation analysis. Overall, our results highlight the involvement of frontal, and parietal cortex mainly but also temporal and occipital cortex, as well as basal ganglia and limbic system areas. According to fMRI studies, these areas seem to play a role in mathematical operations as well as in cognitive control and motivation (Arsalidou et al. 2017).

Math Fluency is based on basic arithmetic operations that depend on recovery of number facts from long-term memory (Andersson 2008), and therefore is expected to pose minimal demands on participants' attentional/WM capacity. Inferior frontal (IF) cortex, medial frontal (MF) cortex and parietal (PSTCG) cortex, mainly from the right hemisphere, are involved in mathematical abilities that are mainly based on automatized processes (Arsalidou et al. 2017). The left IPS plays also a central role in basic quantitative representation (Dehaene et al. 2004) and in addition and subtraction (Arsalidou and Taylor 2011), representing the basis of the Math Fluency test. In addition, the left frontoparietal network (MF cortex, IPS) might have been recruited to deal with the increased attentional effort required by the time constraint imposed by the test. Reduced attentional resources might explain why the left MF area shows lower volume in children with mathematical learning disorder (Rotzer et al. 2008) and reduced left IPS gray matter in children with math anxiety (Hartwright et al. 2018).

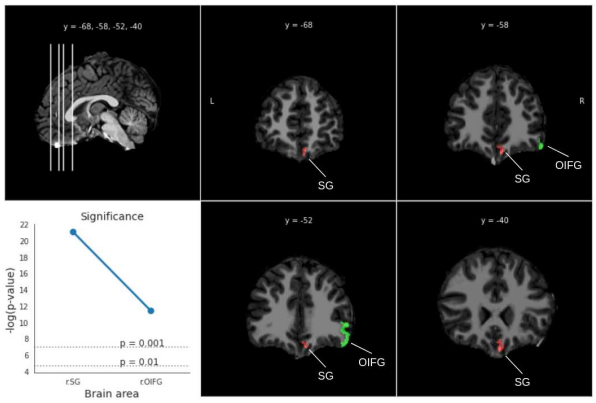

(a) Results for the applied problems test.

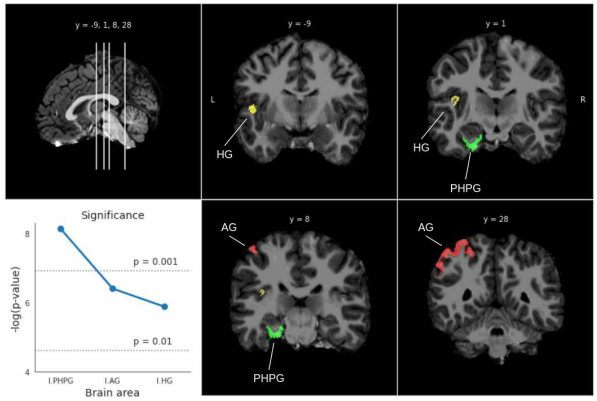

(b) Results for the concepts test.

Fig. 5: Significant areas for applied problems and concepts tests with corresponding plots of the logarithmic p-values for each area.

Calculation is based on the quick activation of the numerical magnitude of Arabic numerals, and arithmetic operations go in increasing order of complexity. Therefore, as with Math Fluency, important areas of the right frontal and parietal lobes involved in numerical automatized processes are also observed (the suborbital sulci, SS and postcentral gyrus, PSTCG), but more complex operations might recruit the posterior cingulate cortex, an area involved in memory retrieval (Rolls 2019). In addition, the involvement of the basal ganglia may be related to important motivational/affective components linked to the performance of this test. Accordingly, the NA has been associated with motivational behavior, and effort regulation (Salamone 1994; Nicola et al. 2005; Salamone et al. 2006). The involvement of the cuneus gyrus can be attributed to the visual recognition of objects but the involvement of the right cuneus gyrus has been related to the approximate calculation in children in previous studies (Kucian et al. 2008).

Applied Problems requires both to hold information in memory and to integrate new information with previous one (Swanson 2011; Pina et al. 2014), and therefore it is expected to impose more demands on executive control capacity than the two previous tests. In accordance, in our case the SG and OIF seem to be implicated. SG is involved in attention control and its functions are integrated with the orbital cortex (Nestor et al. 2015). Liu et al. 2019 observed bilateral implication of the IF gyrus and the SG in arithmetic principles versus computation. Additionally, previous studies showed the involvement of the frontal lobe, specifically bilateral activation of the IF gyri, in mathematical word problems (Prabhakaran et al. 2001). Studies with larger sample sizes, and thus with greater statistical power, are needed to confirm the bilateral activation of these areas in sMRI with the presented methodology.

Finally, the Concepts test assesses the mathematical knowledge (e.g., formulas and terms) and quantitative reasoning. Poor performance on this test is expected when participants show limited vocabulary or insufficient conceptual development (Pina et al. 2015). Accordingly, brain areas involved in this test are lateralized in the left hemisphere, which could reflect a language mediation role (Grabner et al. 2007). Concretely, PHPG participates in remembering facts and rules (Squire et al. 2004) and this area has been proposed to maintain memory representations during the tests (Rivera et al. 2005). The left AG located near the IPS has been related to the language required in some arithmetic operations that use verbal coding or are based on verbally stored knowledge (Grabner et al. 2007). Finally, an important result is the involvement of HG which corresponds to the primary auditory cortex. This area was expected because only for this test were the statements read aloud, and just a drawing was available for each test item. Thus, children needed to be attentive to verbal information.

Our results involve different brain areas depending on the processes required by the different mathematical abilities, and the main areas observed agree with those observed in both functional and structural MRI studies. However, the present study has addressed the issue from a broader and novel perspective. First, we have used an ample range of mathematical tests that differ not only in the specific mathematical abilities, but also in the degree of complexity the arithmetic operations convey and the demands on participants' mental-attentional capacity. This makes the present study an important contribution to better understanding the brain areas that better predict the diverse skills required when people face mathematical facts. Also, despite the sample used here might be rather small (although clearly superior

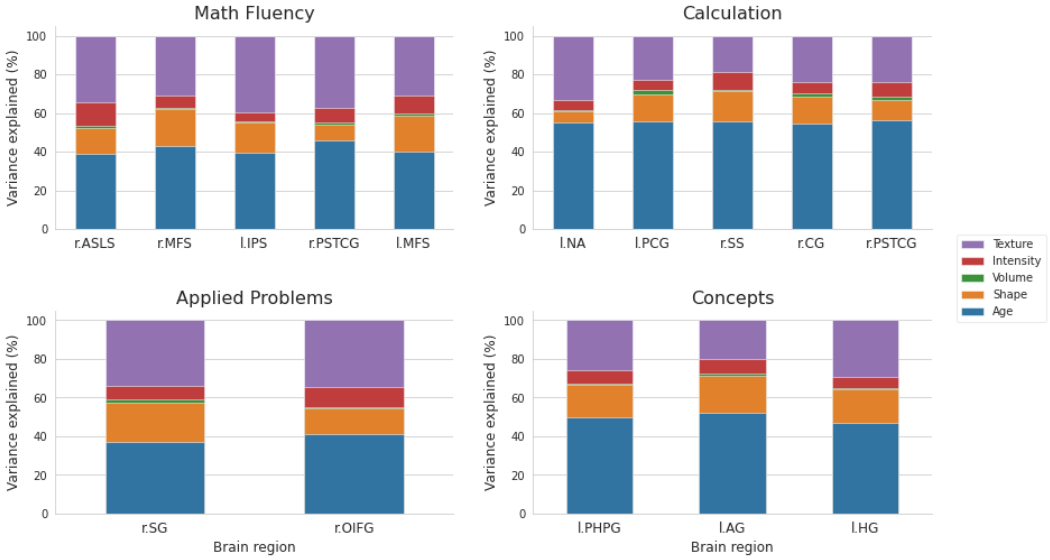

Fig. 6: Percentage of variance explained by groups of radiomics features per area. Note the smaller size of volume (green) compared with shape (orange) or texture (purple) features.

to other neuroimaging approaches), to the best of our knowledge, this is the first study that analyzes mathematical performance in school aged children with radiomics through sMRI images. The open-sourced radiomics-based analysis proposed in this study can be easily automated and therefore potentially used by researchers and clinicians to make the most of radiological studies.

References

Andersson, U. (2008). "Working memory as a predictor of written arithmetical skills in children: The importance of central executive functions". In: *British Journal of Educational Psychology* 78.2, pp. 181–203. DOI: 10.1348/000709907X209854.

Arsalidou, M., Pawliw-Levac, M., Sadeghi, M., and Pascual-Leone, J. (2017). "Brain areas associated with numbers and calculations in children: Meta-analyses of fMRI studies". In: *Developmental Cognitive Neuroscience* 30, pp. 239 –250. DOI: 10.1016/j.dcn.2017.08.002.

Arsalidou, M. and Taylor, M. (2011). "Is 2+2=4? Meta-analyses of brain areas needed for numbers and calculations". In: *NeuroImage* 54, pp. 2382–2393. DOI: 10.1016/j.neuroimage.2010.10.009.

Chaddad, A., Desrosiers, C., Hassan, L., and Tanougast, C. (2017). "Hippocampus and amygdala radiomic biomarkers for the study of autism spectrum disorder". In: *BMC Neuroscience* 18. DOI: 10.1186/s12868-017-0373-0.

Cui, L.-B., Fu, Y.-F., Liu, L., Wu, X.-S., Xi, Y.-B., Wang, H.-N., Qin, W., and Yin, H. (2020). "Baseline structural and functional magnetic resonance imaging predicts early treatment response in schizophrenia". In: *European Journal of Neuroscience*. DOI: 10.1111/ejn.15046.

Dehaene, S., Molko, N., Cohen, L., and Wilson, A. J. (2004). "Arithmetic and the brain". In: *Current Opinion in Neurobiology* 14, pp. 218–224. DOI: 10.1016/j.conb.2004.03.008.

Destrieux, C., Fischl, B., Dale, A., and Halgren, E. (2010). "Automatic parcellation of human cortical gyri and sulci using standard anatomical nomenclature". In: *NeuroImage* 53, pp. 1–15. DOI: 10.1016/j.neuroimage.2010.06.010.

Diamantopoulou, S., Pina, V., Valero-Garcia, A. V., González-Salinas, C., and Fuentes, L. J. (2012). "Validation of the Spanish version of the Woodcock-Johnson mathematics achievement tests for children aged 6 to 13". In: *Journal of Psychoeducational Assessment* 30.5, pp. 466–477. DOI: 10.1177/0734282912437531.

Eriksson, J., Vogel, E., Lansner, A., Bergström, F., and Nyberg, L. (2015). "Neurocognitive Architecture of Working Memory". In: *Neuron* 88, pp. 33–46. DOI: 10.1016/j.neuron.2015.09.020.

Fischl, B., Kouwe, A. van der, Destrieux, C., Halgren, E., Ségonne, F., Salat, D., Busa, E., Seidman, L., Goldstein, J., Kennedy, D., Caviness, V., Makris, N., Rosen, B., and Dale, A. (2004). "Automatically parcellating the human cerebral cortex." In: *Cerebral Cortex* 14 1, pp. 11–22. DOI: 10.1093/cercor/bhg087.

Fritz, A., Haase, V. G., and Rasanen, P (2019). *International handbook of mathematical learning difficulties*. Springer.

Gazzaley, A., Rissman, J., and D'Esposito, M. (2004). "Functional connectivity during working memory maintenance". In: *Cognitive, Affective, & Behavioral Neuroscience* 4, pp. 580–599. DOI: 10.3758/CABN.4.4.580.

Gillies, R., Kinahan, P., and Hricak, H. (2016). "Radiomics: Images Are More than Pictures, They Are Data". In: *Radiology* 278, pp. 563 –577. DOI: 10.1148/radiol.2015151169.

Grabner, R., Ansari, D., Reishofer, G., Stern, E., Ebner, F., and Neuper, C. (2007). "Individual differences in mathematical competence predict parietal brain activation during mental calculation". In: *NeuroImage* 38, pp. 346–356. DOI: 10.1016/j.neuroimage.2007.07.041.

Griethuysen, J. van, Fedorov, A., Parmar, C., Hosny, A., Aucoin, N., Narayan, V., Beets-Tan, R., Fillion-Robin, J.-C., Pieper, S., and Aerts, H. J. (2017). "Computational Radiomics System to Decode the Radiographic Phenotype." In: *Cancer research* 77 21, e104–e107. DOI: 10.1158/0008-5472.CAN-17-0339.

Guerrisi, A., Loi, E., Ungania, S., Russillo, M., Bruzzaniti, V., Elia, F., Desiderio, F., Marconi, R., Solivetti, F. M., and Strigari, L. (2020). "Novel cancer therapies for advanced cutaneous melanoma: The added value of radiomics in the decision making process–A systematic review". In: *Cancer Medicine* 9.5, pp. 1603–1612. DOI: 10.1002/cam4.2709.

Hartwright, C. E., Looi, C. Y., Sella, F., Inuggi, A., Santos, F. H., González-Salinas, C., Santos, J. M. G., Kadosh, R. C., and Fuentes, L. J. (2018). "The neurocognitive architecture of individual differences in math anxiety in typical children". In: *Scientific Reports* 8, p. 8500. DOI: 10.1038/s41598-018-26912-5.

Houdé, O., Rossi, S., Lubin, A., and Joliot, M. (2010). "Mapping numerical processing, reading, and executive functions in the developing brain: an fMRI meta-analysis of 52 studies including 842 children." In: *Developmental Science* 13 6, pp. 876–85. DOI: 10.1111/j.1467-7687.2009.00938.x.

Huang, Y., Liu, Z., He, L., Chen, X., Pan, D., Ma, Z., Liang, C., Tian, J., and Liang, C. (2016). "Radiomics Signature: A Potential Biomarker for the Prediction of Disease-Free Survival in Early-Stage (I or II) Non-Small Cell Lung Cancer." In: *Radiology* 281 3, pp. 947–957. DOI: 10.1148/radiol.2016152234.

Kaufman, A. S. and Kaufman, N. L. (1990). *Manual for the Kaufman brief intelligence test*. MN: American Guidance Service.

Kucian, K., Aster, M. von, Loenneker, T., Dietrich, T., and Martin, E. (2008). "Development of Neural Networks for Exact and Approximate Calculation: A fMRI Study". In: *Developmental Neuropsychology* 33, pp. 447 –473.

Larroza, A., Bodí, V., Moratal, D., et al. (2016). "Texture analysis in magnetic resonance imaging: review and considerations for future applications". In: *Assessment of cellular and organ function and dysfunction using direct and derived MRI methodologies*, pp. 75–106. DOI: 10.5772/64641.

Liu, J., Yuan, L., Chen, C., Cui, J., and Zhou, X. (2019). "The Semantic System Supports the Processing of Mathematical Principles". In: *Neuroscience* 404, pp. 102–118. DOI: 10.1016/j.neuroscience.2019.01.043.

Lowekamp, B. C., Chen, D., Ibáñez, L., and Blezek, D. (2013). "The Design of SimpleITK". In: *Frontiers in Neuroinformatics* 7, p. 45. DOI: 10.3389/fninf.2013.00045.

Nestor, P., Nakamura, M., Niznikiewicz, M., Levitt, J., Newell, D., Shenton, M., and McCarley, R. (2015). "Attentional Control and Intelligence: MRI Orbital Frontal Gray Matter and Neuropsychological Correlates". In: *Behavioural Neurology* 2015.

Nicola, S., Taha, S., Kim, S. W., and Fields, H. (2005). "Nucleus accumbens dopamine release is necessary and sufficient to promote the behavioral response to reward-predictive cues". In: *Neuroscience* 135, pp. 1025–1033. DOI: 10.1016/j.neuroscience.2005.06.088.

Park, Y., Choi, D., Lee, J., and Bang, M. (2020). "Differentiating patients with schizophrenia from healthy controls by hippocampal subfields using radiomics". In: *Schizophrenia research*. DOI: 10.1016/j.schres.2020.09.009.

Peters, L. and Smedt, B. D. (2017). "Arithmetic in the developing brain: A review of brain imaging studies". In: *Developmental Cognitive Neuroscience* 30, pp. 265 –279. DOI: 10.1016/j.dcn.2017.05.002.

Pina, V., Castillo, A., Kadosh, R. C., and Fuentes, L. J. (2015). "Intentional and automatic numerical processing as predictors of mathematical abilities in primary school children". In: *Frontiers in Psychology* 6. DOI: 10.3389/fpsyg.2015.00375.

Pina, V., Fuentes, L. J., Castillo, A., and Diamantopoulou, S. (2014). "Disentangling the effects of working memory, language, parental education, and non-verbal intelligence on children's mathematical abilities". In: *Frontiers in Psychology* 5, p. 415. DOI: 10.3389/fpsyg.2014.00415.

Prabhakaran, V., Rypma, B., and Gabrieli, J. (2001). "Neural substrates of mathematical reasoning: a functional magnetic resonance imaging study of neocortical activation during performance of the necessary arithmetic operations test." In: *Neuropsychology* 15 1, pp. 115–27. DOI: 10.1037//0894-4105.15.1.115.

Raisi-Estabragh, Z., Izquierdo, C., Campello, V. M., Martín-Isla, C., Jaggi, A., Harvey, N., Lekadir, K., and Petersen, S. (2020). "Cardiac magnetic resonance radiomics: basic principles and clinical perspectives". In: *European Heart Journal Cardiovascular Imaging* 21, pp. 349 –356. DOI: 10.1093/ehjci/jeaa028.

Rivera, S., Reiss, A., Eckert, M., and Menon, V. (2005). "Developmental changes in mental arithmetic: evidence for increased functional specialization in the left inferior parietal cortex." In: *Cerebral Cortex* 15 11, pp. 1779–90. DOI: 10.1093/cercor/bhi055.

Rolls, E. (2019). "The cingulate cortex and limbic systems for emotion, action, and memory". In: *Brain Structure & Function* 224, pp. 3001 –3018. DOI: 10.1007/s00429-019-01945-2.

Rotzer, S., Kucian, K., Martin, E., Aster, M., Klaver, P., and Loenneker, T. (2008). "Optimized voxel-based morphometry in children with developmental dyscalculia". In: *NeuroImage* 39, pp. 417–422. DOI: 10.1016/j.neuroimage.2007.08.045.

Salamone, J. (1994). "The involvement of nucleus accumbens dopamine in appetitive and aversive motivation". In: *Behavioural Brain Research* 61, pp. 117–133. DOI: 10.1016/0166-4328(94)90153-8.

Salamone, J., Correa, M., Farrar, A., and Mingote, S. (2006). "Effort-related functions of nucleus accumbens dopamine and associated forebrain circuits". In: *Psychopharmacology* 191, pp. 461–482. DOI: 10.1007/s00213-006-0668-9.

Sánchez-Pérez, N., Castillo, A., López-López, J., Pina, V., Puga, J. L., Campoy, G., González-Salinas, C., and Fuentes, L. J. (2018). "Computer-Based Training in Math and Working Memory Improves Cognitive Skills and Academic Achievement in Primary School Children: Behavioral Results". In: *Frontiers in Psychology* 8, p. 2327. DOI: 10.3389/fpsyg.2017.02327.

Sánchez-Pérez, N., Inuggi, A., Castillo, A., Campoy, G., García-Santos, J. M., González-Salinas, C., and Fuentes, L. J. (2019). "Computer-Based Cognitive Training Improves Brain Functional Connectivity in the Attentional Networks: A Study With Primary School-Aged Children". In: *Frontiers in Behavioral Neuroscience* 13, p. 247. DOI: 10.3389/fnbeh.2019.00247.

Squire, L., Stark, C., and Clark, R. E. (2004). "The medial temporal lobe." In: *Annual Review of Neuroscience* 27, pp. 279–306. DOI: 10.1146/annurev.neuro.27.070203.144130.

Sun, H., Chen, Y., Huang, Q., Lui, S., Huang, X., Shi, Y., Xu, X., Sweeney, J., and Gong, Q. (2018). "Psychoradiologic Utility of MR Imaging for Diagnosis of Attention Deficit Hyperactivity Disorder: A Radiomics Analysis." In: *Radiology* 287 2, pp. 620–630. DOI: 10.1148/radiol.2017170226.

Swanson, H. (2011). "Intellectual growth in children as a function of domain specific and domain general working memory subgroups". In: *Intelligence* 39, pp. 481–492. DOI: 10.1016/j.intell.2011.10.001.

Tustison, N., Cook, P., Klein, A., Song, G., Das, S., Duda, J. T., Kandel, B., Strien, N. V., Stone, J. R., Gee, J., and Avants, B. (2014). "Large-scale evaluation of ANTs and FreeSurfer cortical thickness measurements". In: *NeuroImage* 99, pp. 166–179. DOI: 10.1016/j.neuroimage.2014.05.044.

Acknowledgements

This work was supported by the Ministry of Economy, Industry and Competitiveness of Spain, grant PSI2017-84556-P (FEDER funds) and by the European Union's Horizon 2020 research and innovation program under grant agreement number 825903 (euCanSHare project). The authors would like to thank the Barcelona Super Computing Centre (BSC-CNS) for the computing resources used in this work.

Author contributions

VP, VMC, and LJF conceptualized and designed the study. JMGS acquired the data. VP, VMC, KL, SS and LJF analyzed and interpreted the data. VP, VMC and LJF wrote the manuscript. VMC, SS and KL prepared the figures. All authors read and approved the final version of the manuscript.

Competing Interests

The authors declare no competing interests.

Data and code availability

The code used for this analysis is publicly available to enhance reproducibility at:

github.com/vicmancr/MathBrainRadiomics. Data will be available upon request to either the first author or the corresponding author.

Supplementary material

Table 3: List of 100 Radiomics features considered during the analysis.

Group	Index	Feature
Shape	1	Elongation
	2	Flatness
	3	LeastAxisLength
	4	MajorAxisLength
	5	Maximum2DDiameterColumn
	6	Maximum2DDiameterRow
	7	Maximum2DDiameterSlice
	8	Maximum3DDiameter
	9	MeshVolume
	10	MinorAxisLength
	11	Sphericity
	12	SurfaceArea
	13	SurfaceVolumeRatio
	14	VoxelVolume
First order	15	10Percentile
	16	90Percentile
	17	Energy
	18	Entropy
	19	InterquartileRange
	20	Kurtosis
	21	Maximum
	22	MeanAbsoluteDeviation
	23	Mean
	24	Median
	25	Minimum
	26	Range
	27	RobustMeanAbsoluteDeviation
	28	RootMeanSquared
	29	Skewness
	30	TotalEnergy
	31	Uniformity
	32	Variance
GLCM	33	Autocorrelation
	34	JointAverage
	35	ClusterProminence
	36	ClusterShade
	37	ClusterTendency
	38	Contrast
	39	Correlation
	40	DifferenceAverage
	41	DifferenceEntropy
	42	DifferenceVariance
	43	JointEnergy
	44	JointEntropy
	45	Imc1
	46	Imc2
	47	Idm
	48	Idmn
	49	Id
	50	Idn
GLCM	51	InverseVariance
	52	MaximumProbability
	53	SumEntropy
	54	SumSquares
GLRLM	55	GrayLevelNonUniformity
	56	GrayLevelNonUniformityNormalized
	57	GrayLevelVariance
	58	HighGrayLevelRunEmphasis
	59	LongRunEmphasis
	60	LongRunHighGrayLevelEmphasis
	61	LongRunLowGrayLevelEmphasis
	62	LowGrayLevelRunEmphasis
	63	RunEntropy
	64	RunLengthNonUniformity
	65	RunLengthNonUniformityNormalized
	66	RunPercentage
	67	RunVariance
	68	ShortRunEmphasis
	69	ShortRunHighGrayLevelEmphasis
	70	ShortRunLowGrayLevelEmphasis
GLSZM	71	GrayLevelNonUniformity
	72	GrayLevelNonUniformityNormalized
	73	GrayLevelVariance
	74	HighGrayLevelZoneEmphasis
	75	LargeAreaEmphasis
	76	LargeAreaHighGrayLevelEmphasis
	77	LargeAreaLowGrayLevelEmphasis
	78	LowGrayLevelZoneEmphasis
	79	SizeZoneNonUniformity
	80	SizeZoneNonUniformityNormalized
	81	SmallAreaEmphasis
	82	SmallAreaHighGrayLevelEmphasis
	83	SmallAreaLowGrayLevelEmphasis
	84	ZoneEntropy
	85	ZonePercentage
	86	ZoneVariance
GLDM	87	DependenceEntropy
	88	DependenceNonUniformity
	89	DependenceNonUniformityNormalized
	90	DependenceVariance
	91	GrayLevelNonUniformity
	92	GrayLevelVariance
	93	HighGrayLevelEmphasis
	94	LargeDependenceEmphasis
	95	LargeDependenceHighGrayLevelEmphasis
	96	LargeDependenceLowGrayLevelEmphasis
	97	LowGrayLevelEmphasis
	98	SmallDependenceEmphasis
	99	SmallDependenceHighGrayLevelEmphasis
	100	SmallDependenceLowGrayLevelEmphasis

The abbreviations stand for Gray Level Co-ocurrence Matrix (GLCM), Gray Level Run Length Matrix (GLRLM), Gray Level Size Zone Matrix (GLSZM) and Gray Level Dependence Matrix (GLDM). Details for interpreting these features as well as their definitions are provided in the PyRadiomics documentation: pyradiomics.readthedocs.io

Figures

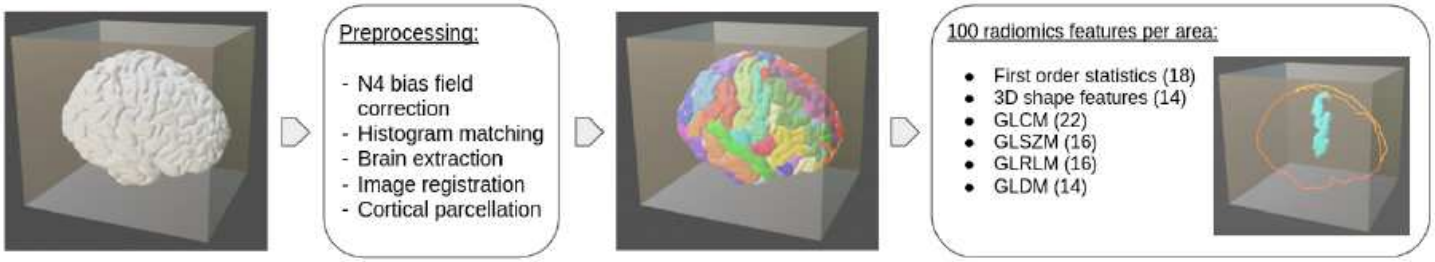

Figure 1

Schematic pipeline for extracting radiomics features from sMRI.

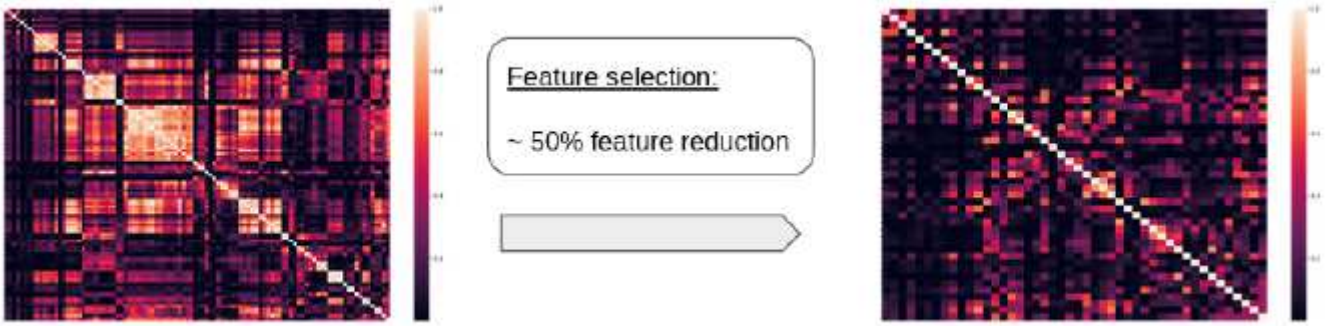

Figure 2

Example of a correlation matrix for radiomics features before and after the feature reduction for a given area, showing signicant reduction in the number of correlated features.

Figure 3

Method pipeline used for computing the resulting errors for each area and for each mathematical test.

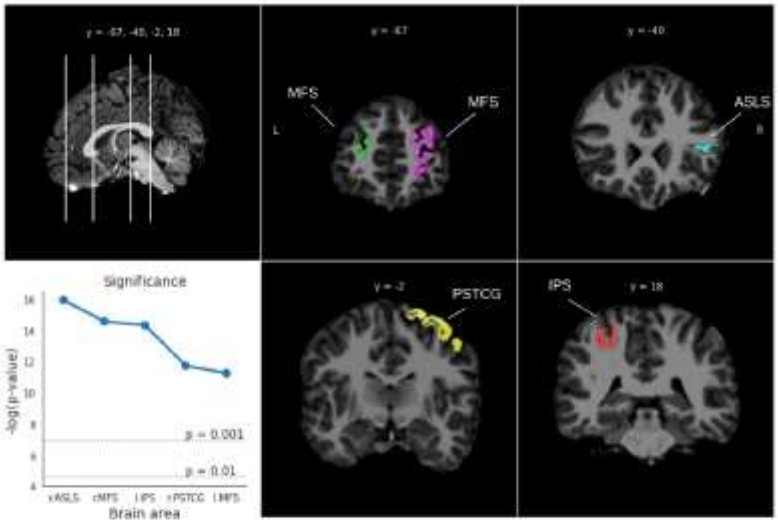

(a) Results for the math fluency test.

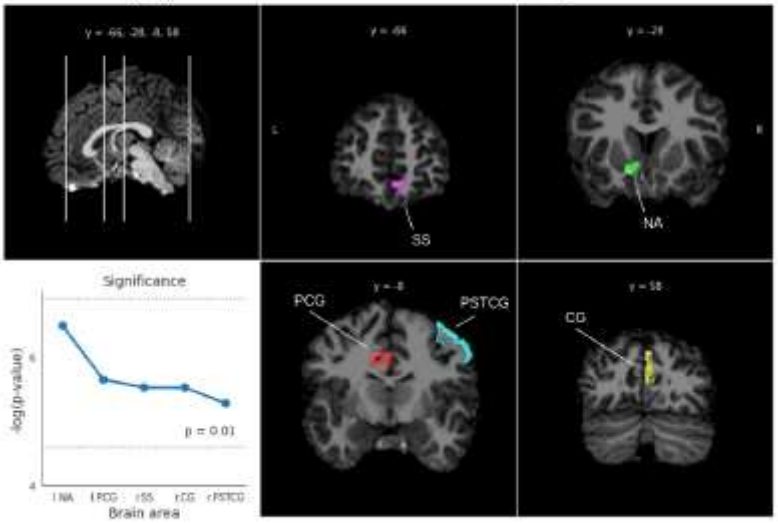

(b) Results for the calculation test.

Figure 4

Signicant areas for math uency and calculation tests with corresponding plots of the logarithmic p-values for each area. The acronyms are dened in Table 2.

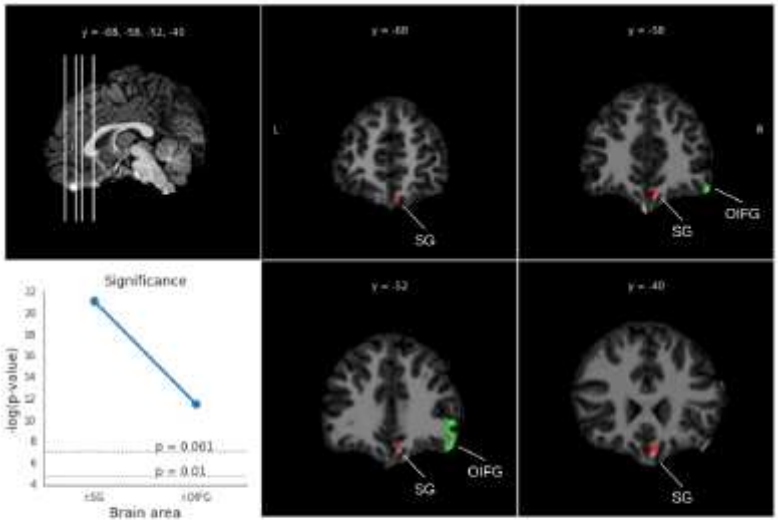

(a) Results for the applied problems test.

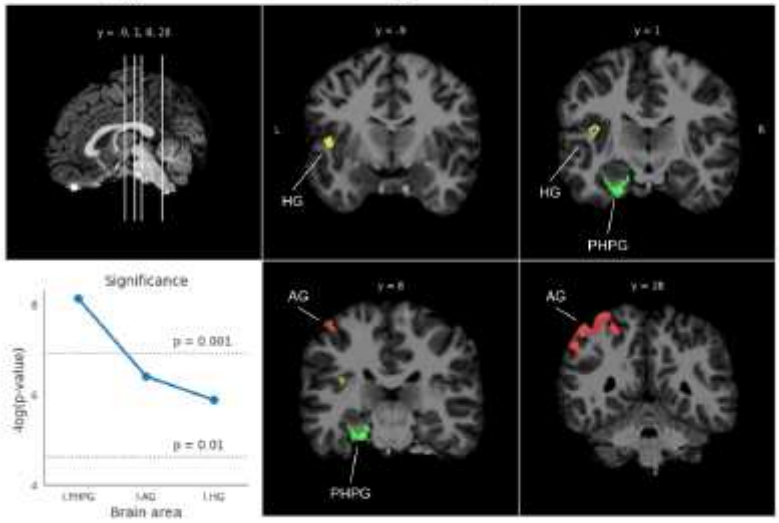

(b) Results for the concepts test.

Figure 5

Signicant areas for applied problems and concepts tests with corresponding plots of the logarithmic p-values for each area.

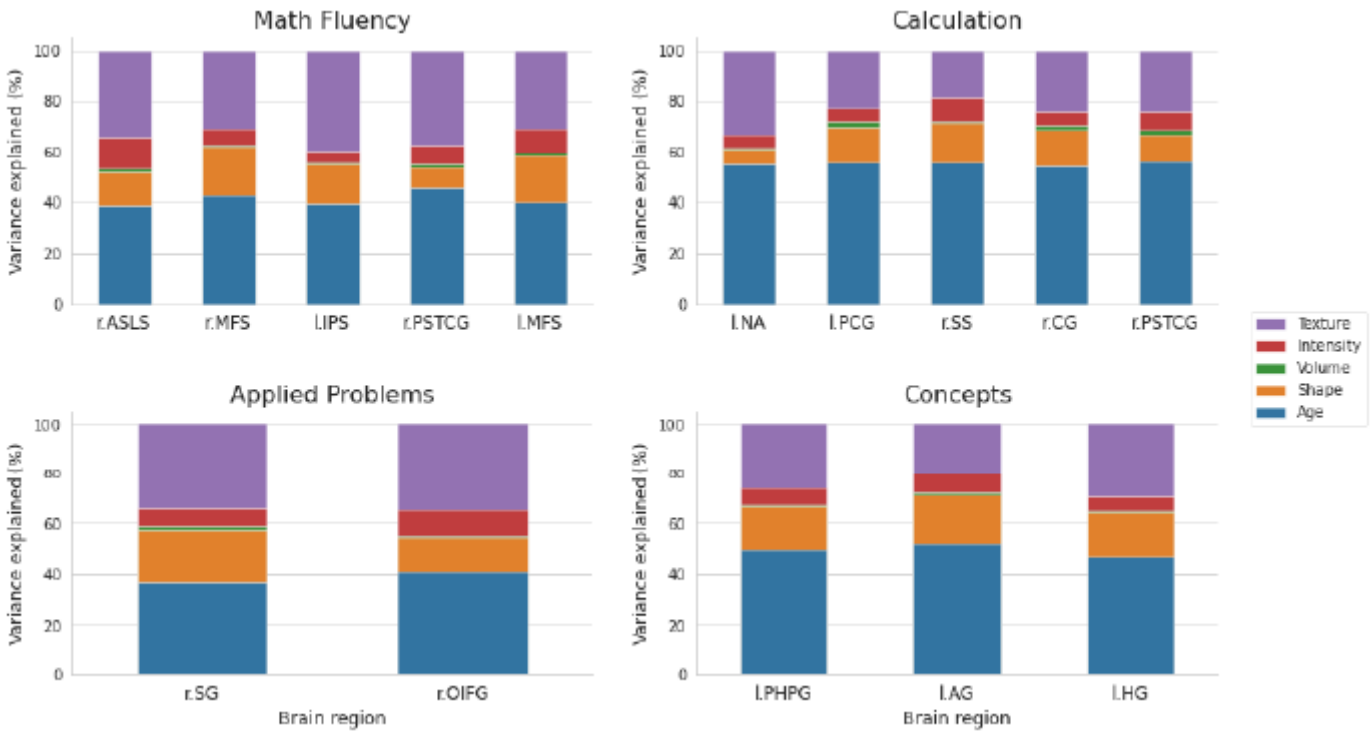

Figure 6

Percentage of variance explained by groups of radiomics features per area. Note the smaller size of volume (green) compared with shape (orange) or texture (purple) features.